Available online at www.sciencedirect.com

ScienceDirect

Procedia CIRP 49 (2016) 94 – 98

www.elsevier.com/locate/procedia

The Second CIRP Conference on Biomanufacturing

Computational Simulation and Experimental Research of Flow Rates in Coaxial Fluids for Fabricating Hydrogel Fibers

Shuai Li[a], Yuanyuan Liu[a,b,*], Change Liu[a], Yu Li[a], Qingxi Hu[a,b]

[a]*Rapid Manufacturing Engineering Center, Shanghai University, Shanghai 200444, China*
[b]*Shanghai Key Laboratory of Intelligent Manufacturing and Robotics, Shanghai University, Shanghai 200072, China*

* Corresponding author. Tel.: +86-21-66133157-8019. *E-mail address:* yuanyuan_liu@shu.edu.cn

Abstract

As one of the biomanufacturing technologies, 3D bioprinting is becoming one effective way to solve the issues in tissue engineered constructs. In order to produce 3D cell-laden scaffolds to overcome the main technological barrier in cell distribution and nutrient supply and better mimic the *in vivo* cellular environment, hydrogel fibers were used to deposit in 3D bioprinting system and obtain the 3D cell-laden hydrogel structures. In the present work, we investigate the effects of flow rates on the dimensions of hydrogel fibers. The volume of fluid model by the computational fluid dynamics software package FLUENT 6.3.26 is applied to obtain the appropriate flow rates to produce hydrogel fibers. Different flow pattern in the coaxial model is obtained. In addition, a coaxial nozzle was used to fabricate hydrogel fibers under various flow rates to know its' effects on the dimension of hydrogel fibers.

Peer-review under responsibility of the scientific committee of The Second CIRP Conference on Biomanufacturing

Keywords: 3D bioprinting; Hydrogel fiber; Flow rate; Coaxial fluids

1. Introduction

Tissue engineering has been a promising field of research for several decades. The appearance of 3D printing offers many solutions in the fields of manufacturing, engineering and medicine. Print biocompatible materials, cells and supporting components into complex 3D functional living tissues has became an effective way to build 3D cell-laden scaffolds. Moreover, one of the main challenges in the 3D bioprinting has been to find materials that are not only compatible with cells and the tissue in host but can also provide the desired mechanical and functional properties [1, 2]. Finally, materials can be printed as tissue substitutes for skin [3], bone regeneration [4] and so on.

Microextrusion [5], inkjet [6], laser assisted printing [7] and microfluidic chip [8] are the main technologies used for printing biological materials. Much recent research has been aimed at using biomaterials combined with microfibrication to realize the 3D biocompatible structures. Hydrogel fibers extruded from microfluidic chip or coaxial nozzle was used to build the 3D cell-laden hydrogel structures. But many hydrogel-based scaffolds lack cell-sized pores and hydrophilia. Such micropores are highly desirable since they supply the cells with oxygen and nutrients and remove waste products. Due to the hydrophobe in the surface of the biomaterials, cells can not adhere to the 3D scaffolds. Thus, cell-laden fibers containing micropores and hydriphilia have become promising applications in the field of 3D bioprinting [9, 10].

The use of coaxial microfluidic to extrude hydrogel fibers offers a method to fabricate 3D cell-laden structures. Jung et al. [11] used glass capillaries to assemble microfluidcis to generate cell-laden microgel. The cells in the inner phase can effectively attach to the outer hydrogel. Oh et al. [12] employed a microfluidic coaxial flow–focusing system to generate cell adhesive chitosan microtubes of controlled sizes. The inner sodium tripolyphosphate (TPP) crosslink with the outer chitosan and the hollow fibers formed. Similarly, Gao et al. [13] used a coaxial nozzle to print hollow calcium alginate filaments. The inner calcium chloride crosslinked with sodium alginate was used to build high strength cell-laden hydrogel 3D structures. Moreover, Onoe et al. [14] fabricated meter-long core-shell Ca-alginate microfibers encapsulating

Peer-review under responsibility of the scientific committee of The Second CIRP Conference on Biomanufacturing
doi:10.1016/j.procir.2015.07.083

extracellular metrices (ECMs) proteins and differentiated cells by using a double-coaxial microfluidic device. More and more research focus on the inside-out crosslinking to obtain hydrogel fibers. But the research of outside-in crosslinking process is still lack, since the outside-in crosslinking is also an important aspect to comprehend the mechanism of hydrogel crosslinking.

In the current work, a coaxial nozzle combined with outside-in crosslinking process was used to investigate the feasibility of fabricating hydrogel fibers. In order to obtain the appropriate flow rates of two-phase used in this work, CFD simulations were performed using VOF model in software package FLUENT 6.3.26. The classic two-phase flow pattern, dripping and jetting were formed under different flow rates. In addition, the effect of flow rates on the dimension of hydrogel fibers was investigated. Results show that the outside-in crosslinking process is similar to the two-phase flow theories.

2. Numerical simulation

In order to ensure the appropriate range of flow rates used in fabricating hydrogel fibers. A 3D model developed using CFD software FLUENT 6.3.26. Mesh generation is one of the most important steps in the preprocess stage. The meshing of the model of the flow field under the domain geometry was established using the software GAMBIT, as shown in Fig.1. The mesh consists of 30278 quad cells and 33980 nodes.

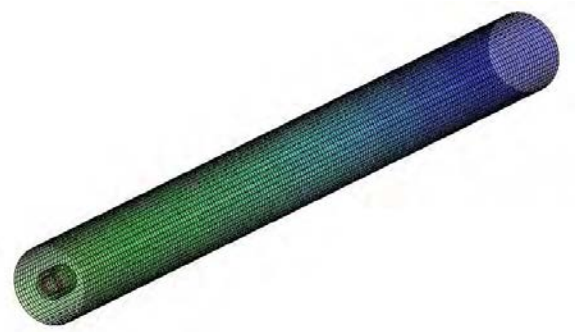

Fig. 1. Schematic of meshed geometry.

Volume of Fluid (VOF) was chosen as the multiphase model. Explicit was selected as the VOF Scheme. In FLUENT, the stability and convergence of computing can be adjusted through Courant number. In general, as the Courant number changes from small to large, the speed of convergence gradually accelerated, but stability decreased. After several attempts, 0.1 was chosen as the Courant number. Not only ensure the convergence, but also guarantee the stability of calculation.

As for convergence criterion, three important aspects need to abide by for iterative convergence [15]. First, all the discretized equations (momentum, energy, etc) are deemed to be converged when they reach a specified tolerance at every nodal location. Second, the numerical solution no longer changes with additional iterations. Third, overall mass, momentum, energy, and scalar balances are obtained. In our calcutions, the numerical computation is considered converged when the residuals of the different variables are lowered by three orders of magnitude. As shown in Fig.2.

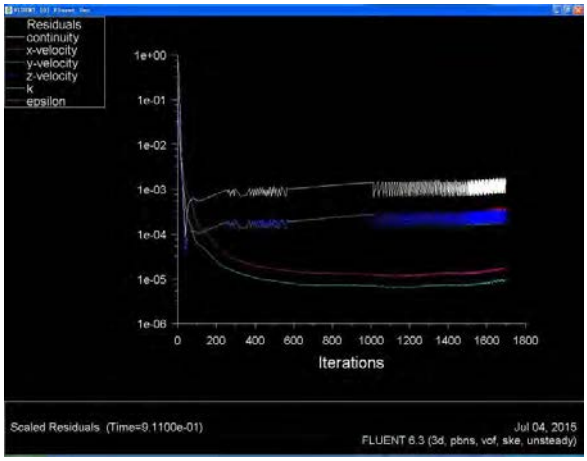

Fig. 2. Residuals of the calculation.

The pressure equation was discretized using PRESTO. The first order up wind method was used for the discretization of the momentum equation, turbulent kinetic energy and turbulent dissipation rate. The volume fraction was reconstructed using the geo-reconstruct method. PISO was used for coupling the pressure-velocity.

In order to find the boundary conditions, a needle was used to extrude the uncrosslinked hydrogel. When the feed rate was around 900 µl min^{-1}, the uncrosslinked hydrogel can be extruded from the needle smoothly without crevice. Thus, the flow rates of inner phase in FLUENT was determined. As for the flow rates of outer phase, 150, 60, and 10 µl min^{-1}, three different flow rates was chosen to simulate the process.

3. Experimental details

3.1. Materials

Sodium alginate and calcium chloride ($CaCl_2$) (purchased from Sinopharm Chemical Reagent CO., Ltd., China) were used to fabricate the hydrogel fibers. Sodium alginate solution was prepared by dissolving Na-Alginate into deionized water and placed in a magnetic stirrer for 10 h at 120 rpm at room temperature to make final Na-Alginate solution with a concentration of 4 % (w/v). Similarly, 5 % (w/v) calcium chloride solution was prepared using deionized water.

3.2. Fabrication of hydrogel fibers

The experimental setup consisted of a coaxial nozzle, with two syringe pumps (TJ-3A, Baoding Longer Precision Pump Co., Ltd., China) for the sodium alginate and $CaCl_2$ solutions. In this research, the coaxial nozzle was fabricated using two fluid dispensing tips with a Y-branch valve, a 19 gauge (680 µm inner diameter (I.D.), 1100 µm outer diameter (O.D.)) inner needle and a 13 gauge (1920 µm I.D., 2400 µm O.D.) stainless outer needle. As shown in Fig.3. The inner needle is

shorted than the outer needle to ensure the completely crosslink inside the coaxial nozzle. The sodium alginate was dispensed from the core section of the coaxial nozzle by a syringe pump, while the calcium chloride solution was dispensed from the sheath section. When the two solutions contacted each other, hydrogel fibers formed.

3.3. Parameter setup

In this research, the main purpose was to investigate the effect of flow rates on the dimensions of hydrogel fibers. Therefore, different flow rates were chosen in our experiment. Base on our many attempts, concentrations of 4% sodium alginate and 5% calcium chloride were preferred to produce hydrogel fibers under different flow rates. The flow rates of alginate and crosslinker were investigated, Thus, two groups of the flow rates can be obtained. In the first group, the flow rate of calcium chloride was fixed, the flow rate of alginate gradually increased. In the other group, vice versa. The arrangement of two-phase flow rates can be seen in Table 1.

Table 1. Arrangement of flow rates.

Group	Fluids	Flow Rates (μl min^{-1})
A	Sodium alginate	700, 800, 900, 1000, 1100
	Calcium chloride	50
B	Sodium alginate	900
	Calcium chloride	30, 40, 50, 60, 70

3.4. Measurements and Statistical analysis

The dimensions and structure of the hydrogel fibers were observed with an optical microscope (EV3020, EASSON, China). The average diameters of the hydrogel fibers were determined by measuring the diameters at five different locations. GraphPad Prism 5 (GraphPad Software, Inc) was used to process the data. The results were expressed as the mean ± standard deviation (SD).

4. Results and discussion

4.1. Fabrication

The crosslinked hydrogel fibers can be extruded from the coaxial nozzle. As shown in Fig.3. The flow rates can be changed by adjusting the feed rates of the syringe pump. Based on the setup in our experiments, two groups of fibers were obtained.

The structures and dimensions of the fibers were determined under an optical microscope. One sample was chosen to show the viability of fabricating crosslinked hydrogel fibers. As shown in Fig.4.

4.2. The choose of flow rates

Three different flow rates were chosen to determine the

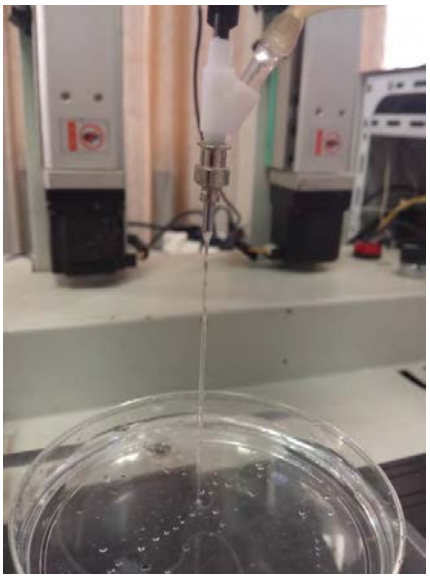

Fig. 3. Extrusion of crosslinked hydrogel fibers from the coaxial nozzle.

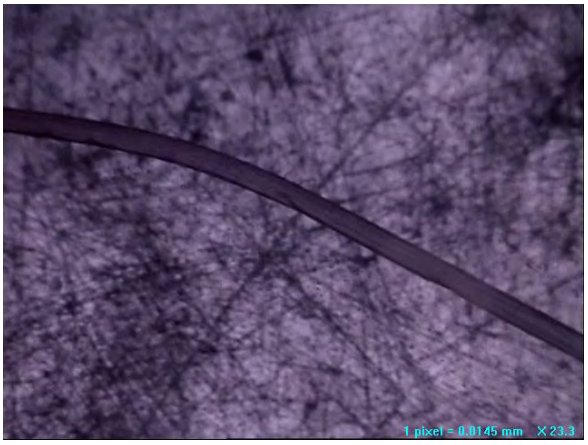

Fig. 4. Microscope imaging of hydrogel fibers.

approprite flow rates range. The dripping flow pattern was generate when the flow rate of caicium chloride was 150 μl min^{-1}, as shown in Fig.5(a). This flow rate is too quick for two-phases to crosslink. Thus, the extruded alginate will crosslinked quickly at the port of the inner needle. And the dripping was obtained. When the flow rate of caicium chloride decrease to 60 μl min^{-1}, the contractive jetting flow pattern was generate, as shown in Fig.5(b). The inner hydrogel can be extruded continuously. The lower calcium chloride flow rate slow down the crosslinking speed , the inner alginate has enough time to be extruded. Thus, the hydrogel fiber can be obtained. In the third case, the outer phase flow rate is too low and the inner phase can be extruded outside like spray at the port of the inner needle, as shown in Fig.5(c).

Based on these analyses, the ideal flow rate of calcium chloride in our research is around 60 μl min^{-1}.

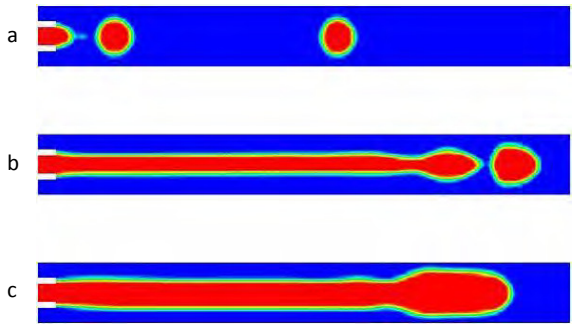

Fig. 5. Different flow contours of alginate: (a) dripping; (b) drag jetting; (c) spray jetting.

4.3. Effect of flow rate on the dimensions of the fibers

After the hydrogel fibers can be extruded from the coaxial nozzle, flow rates can be adjusted to investigate the effect of flow rates on the dimension of hydrogel fibers. Here, we divided the flow rates into two groups: in the first group, the sodium alginate flow rate were set at 700, 800, 900, 1000, and 1100 µl min^{-1} while the calcium chloride flow rate was fixed at 50 µl min^{-1}; in the other group, the sodium alginate flow rate was fixed at 900µl min^{-1} and the calcium chloride flow rates were set at 30, 40, 50, 60, and 70 µl min^{-1}.

Fig.6 shows the quantitative results from the experiments. For the first group fibers, the diameter of the hydrogel fibers obtained from experiment increased from 0.376 ± 0.010 mm to 0.720 ± 0.017 mm, as the flow rate of alginate was increased from 700 to 1100 µl min^{-1} while fixed the flow rate of calcium chloride at 50µl min^{-1}. In contrast, for the other group, the diameter decreased from 0.631 ± 0.028 mm to 0.435 ± 0.013 mm, as the flow rate of calcium chloride was increased from 30 to 70 µl min^{-1} while fixed the flow rate of alginate at 50 µl min^{-1}.

In the first group, the diameter of hydrogel fibers gradually increased due to the inertial forces from the alginate. When the flow rate of alginate was 1100 µl min^{-1}, the diameter of hydrogel fibers even exceed the inner diameter of inner needle. In the second group, the decrease of diameter was caused by the crosslinking shrinkage and the drag force of outer phase. The hydrogel will shrink during the gelation process [16-18]. The content of Ca^{2+} is increase while the flow rate of calcium chloride is increase, more and more divalent ions can crosslink with alginate. Thus the shrinkage degree will increase. In the other hand, as a result of contact, the drag force between two phases will increase while the flow rate of calcium chloride is increase. Thus, the diameter of hydrogel fiber decreased while the flow rate of calcium chloride was increase. One can noticed that when the flow rate of $CaCl_2$ was 30 µl min^{-1}, the diameter of hydrogel fibers was approximately the inner diameter of inner needle. This is similar to the case of high alginate flow rate.

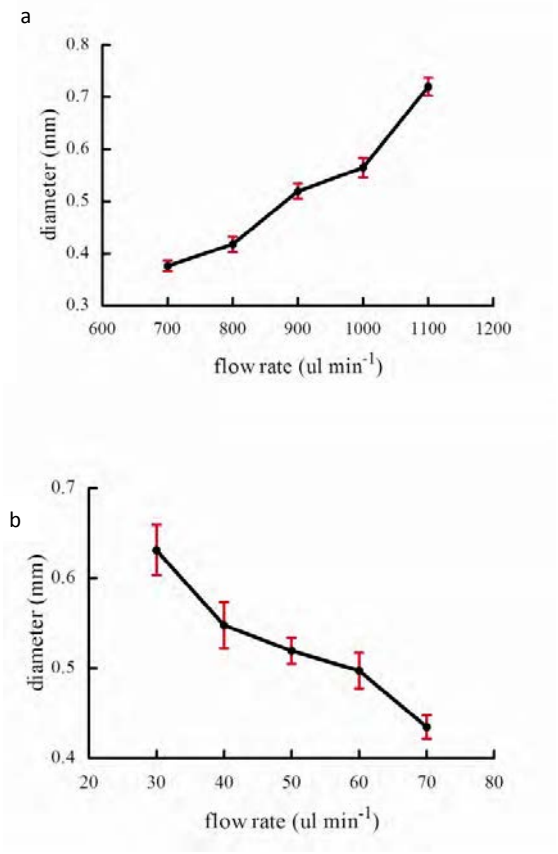

Fig. 6. The effect of flow rates on dimension of hydrogel fibers: (a) fix the flow rate of $CaCl_2$ and gradually increase the flow rate of sodium alginate; (b) fix the flow rate of sodium alginate and gradually increase the flow rate of $CaCl_2$.

5. Conclusion

The current work aimed to investigate the relationship of dimension of hydrogel fibers and two-phase flow rates. CFD simulations were performed using VOF model in software package FLUENT 6.3.26 to know the appropriate flow rates of two-phase used in this work. Moreover, a coaxial nozzle was use to fabricate hydrogel fibers with different dimension under various flow rates. From the study, the diameter of hydrogel fibers was found to be increased with an increase in flow rate of the alginate and decreased with an increase in flow rate of the calcium chloride. The inertial forces from alginate was the dominant factor for the increase of hydrogel fibers diameter, the crosslinking shrinkage and drag forces from calcium chloride caused the decrease of diameter. These process is similar to the classic two-phase flow theories to some extent [19].

Acknowledgements

The authors acknowledge support from the National Natural Science Foundation of China (Grant Nos. 51375292 and 51475281) and the National Natural Science Funds for Young Scholar (Grant Nos. 51105239).

References

[1] Murphy SV, Atala A. 3D bioprinting of tissues and organs. Nat Biotechnol. 2014;32(8):773-785.
[2] Ozbolat IT. Bioprinting scale-up tissue and organ constructs for transplantation. Trends Biotechnol. 2015;33(7):395-400.
[3] Pereira RF, Barrias CC, Granja PL, Bartolo PJ. Advanced biofabrication strategies for skin regeneration and repair. Nanomedicine. 2013;8(4):603-621.
[4] Nguyen LH, Annabi N, Nikkhah M, Bae H, Binan L, Park S, Kang Y, Yang Y, Khademhosseini A. Vascularized bone tissue engineering: approaches for potential improvement. Tissue Eng Part B Rev. 2012;18(5):363-382.
[5] Luo Y, Lode A, Gelinsky M. Direct plotting of three-dimensional hollow fiber scaffolds based on concentrated alginate pastes for tissue engineering. Adv Healthc Mater. 2013;2(6):777-783.
[6] Wu W, DeConinck A, Lewis JA. Omnidirectional printing of 3D microvascular networks. Adv Mater. 2011;23(24):H178-H183.
[7] Guillotin B, Souquet A, Catros S, Duocastella M, Pippenger B, Bellance S, Bareille R, Remy M, Bordenave L, Amedee J, Guillemot F. Laser assisted bioprinting of engineered tissue with high cell density and microscale organization. Biomaterials. 2010;31(28):7250-7256.
[8] Yajima Y, Yamada M, Yamada E, Iwase M, Seki M. Facile fabrication processes for hydrogel-based microfluidic devices made of natural biopolymers. Biomicrofluidics. 2014;8:024115.
[9] Mohanty S, Larsen LB, Trifol J, Szabo P, Burri HV, Canali C, Dufva M, Emneus J, Wolff A. Fabrication of scalable and structured tissue engineering scaffolds using water dissolvable sacrificial 3D printed moulds. Mater Sci Eng C Mater Biol Appl. 2015;55:569-578.
[10] Sousa I, Mendes A, Pereira RF, Bártolo PJ. Collagen surface modified poly(ε-caprolactone) scaffolds with improved hydrophilicity and cell adhesion properties. Mater Lett. 2014;134:263-267.
[11] Jung J, Kim K, Choi SC, Oh J. Microfluidics-assisted rapid generation of tubular cell-laden microgel inside glass capillaries. Biotechnol Lett. 2014;36(7):1549-1554.
[12] Oh J, Kim K, Won SW, Cha C, Gaharwar AK, Selimovic S, Bae H, Lee KH, Lee DH, Lee SH, Khademhosseini A. Microfluidic fabrication of cell adhesive chitosan microtubes. Biomed Microdevices. 2013;15(3):465-472.
[13] Gao Q, He Y, Fu JZ, Liu A, Ma L. Coaxial nozzle-assisted 3D bioprinting with built-in microchannels for nutrients delivery. Biomaterials. 2015;61:203-215.
[14] Onoe H, Okitsu T, Itou A, Kato-Negishi M, Gojo R, Kiriya D, Sato K, Miura S, Iwanaga S, Kuribayashi-Shigetomi K, Matsunaga YT, Shimoyama Y, Takeuchi S. Metre-long cell-laden microfibres exhibit tissue morphologies and functions. Nat Mater. 2013;12(6):584-590.
[15] Tu J, Yeoh G, Liu C. Chapter 5-CFD solution Analysis-Essentials. (2013):177-217.
[16] Kim H. A kinetic study on calcium alginate bead formation. 1990;7(1):1-6.
[17] Li S, Liu Y, Li Y, Zhang Y, Hu Q. Computational and experimental investigations of the mechanisms used by coaxial fluids to fabricate hollow hydrogel fibers. Chemical Engineering and Processing: Process Intensification. 2015;95(0):98-104.
[18] Chrastil J. Gelation of calcium alginate. Influence of rice starch or rice flour on the gelation kinetics and on the final gel structure. J Agr Food Chem. 1991;39(5):874-876.
[19] Guillot P, Colin A, Utada AS, Ajdari A. Stability of a jet in confined pressure-driven biphasic flows at low reynolds numbers. Phys Rev Lett. 2007;99(10):104502.